Efficiency Assessment for Crop Classification Using Multi-Sensor Data in Google Earth Engine

Farhad Ullah[1], Sawaid Abbas[1,2,*], Muhammad Usman[3], Aftab Ameen[1], Zulfiqar Ali Abbas[1], Syed Muhammad Irteza[4], Sami Ullah Khan[5]

[1]Smart Sensing for Climate and Development, Center for Geographical Information System, University of the Punjab, Lahore, Pakistan

[2]Department of Land Surveying and Geo-Informatics, The Hong Kong Polytechnic University, Hong Kong SAR

[3]Interdisciplinary Research Center for Aviation and Space Exploration, King Fahd University of Petroleum and Minerals, Dhahran, Saudi Arabia

[4]Punjab Information Technology Board, Lahore

[5]Urban Unit, Lahore

*Correspondence: sawaid.gis@pu.edu.pk (S.A); sawaid.abbas@connect.polyu.hk Citation | **Citation |** Ullah. F, Abbas. S, Usman. M, Ameen. A, Abbas. Z. A, Irteza. M. S, Khan. S. U, "Efficiency Assessment for Crop Classification Using Multi-Sensor Data in Google Earth Engine", IJIST, Special Issue pp 294-304, June 2024

Received | June 03, 2024; **Revised |** June 07, 2024; **Accepted |** June 13, 2024; **Published |** June 19, 2024.

Accurate mapping of agricultural lands and crop distribution are critical for food security, sustainable development, and policymakers. In this research, agricultural crops were classified using multi-sensor images of Sentinel-1 and Sentinel-2 in Rahim Yar Khan district of Pakistan. The study used the cloud computing platform, Google Earth Engine (GEE), and compared the classification performance of the Random Forest (RF) algorithm using the Sentinel-1 (VV, HV, and HV+VV), Sentinel-2, and integration of the datasets. Ground truth information developed through field surveys and high-resolution images were used as reference samples for training and validation. The fusion of Sentinel-1 and Sentinel-2 data increase the features for better classification of crop types. Post-processing procedures guaranteed that maps were visually clear and devoid of noise, allowing for precise crop mapping and land cover land use categorization. The classification findings showed that crop pixels were effectively classified, with high accuracy for classes including sugarcane, cotton, rice and water bodies. The RF classifier with the fused data produced the highest accuracy (overall accuracy 93%, and Kappa coefficient 90%), followed by the multispectral Sentinel-2 (89 %), Sentinal-1 VV+VH (72%), Sentinel – 1 VH (66 %), and Sentinel – 1 VV (62%). The study highlights the importance of data integration to increase the classification accuracy of major crops (sugarcane, cotton, and rice) in the region. While some classes demonstrated exceptional classification accuracy, others (such as Orchard) indicated need for improvement for further refinement in categorization procedures and approaches. Overall, the study provides useful insights into the use of multi-sensor remote sensing data in agricultural monitoring and decision-making processes.

Keywords: Machine learning, Crop classification, Sentinel-1, Sentinel-2, Google Earth Engine.

Introduction:

The number of people facing hunger in the Asia and Pacific region has reached to 375.8 million in 2020 [1]. This situation is exacerbated as 1.1 billion did not have access to adequate food which presents a bleak picture of food security. In such scenarios, accurate and timely quantification of agricultural crops and their geographical distribution are critical for ensuring food security [2]. Crop mapping is also helpful as an important aspect of crop production forecast and agricultural statistics [3] to assess food demands. Satellite remote sensing has enabled in-season satellite-based crop classifications [4], [5]using multispectral imagery [6].

In June 2015, a high resolution (10 m) remote sensing satellite, Sentinel-2, was launched by the European Space Agency (ESA). The mission consists of two identical satellites, Sentinel-2A and Sentinel-2B, each satellite returns every ten days, giving the constellation a five-day revisit period. The sensor, multispectral instrumentation (MSI) on-board Sentinel-2 provided multispectral data with 13 spectra bands in the visible, near-infrared, and shortwave infrared regions of the spectrum [7], [8]. Despite the higher temporal frequency of observations, the optical data often impeded due to the inability of optical radiation to penetrate through clouds that create gaps in time series observations [9] and can decrease the accuracy of crop type identification [10], [11]. In the areas with frequent cloud cover, the microwave remote sensing can compensate for missing temporal information as well as provide additional information for land cover land use (LCLU) classification. The microwave penetrates through clouds without any substantial interference in its signal as its wavelengths are far greater than those of typical cloud particles[12]. Synthetic Aperture Radar (SAR), microwave-based imaging can enhance our understand about earth resources [13]. Since the launch of the Sentinel-1 mission by the ESA, SAR based applications of crop classification has increase. Previously Sentinel-1A and -1B, both were functioning and providing observations after every 6 days, but nowadays only Sentinel-1A is operational that can provide repeat coverage of earth every 12 days [12]. In order to develop dense time series and extract information from the integrated datasets, this study used the Google Earth Engine (GEE), a non-profit cloud computing platform for geographic spatial analysis [14] . It has been widely used in large-scale remote sensing applications, including forest monitoring, crop yield estimation, and crop mapping [15]. The variety of dataset in the GEE and its derivatives provide a stable data source for accurate crop extraction using multi-source remote sensing images. The main objective of this study is to integrate Sentinel-1 and Sentinel-2 satellite images in Rahim Yar Khan district and compares the classification performance of Random Forest algorithm using the Sentinel-1(VV, HV and VV+HV), Sentinel-2, and integration of datasets.

Material and Methods:

Description of the Study Area:

The Rahim Yar Khan district is situated between 60°44' and 70°02' East and 27°41' and 29°15' North (Figure 1). It covers an area of 11,880 km^2. The district experiences extremely hot and dry summers, with recorded temperatures ranging from 6.8°C to 49.7°C, and average annual rainfall of 165 mm. The district is divided into three main sections: the river region, the irrigated region, and the Cholistan region. The irrigated area lies to the southwest of the district's river area, adjacent to the Indus and Panjnad rivers, with elevations between 150 and 200 meters above sea level. The desert, known as Cholistan, is situated in the southeast corner. Sugarcane, wheat, and cotton are the primary crops grown in the region, while major industries include textile spinning, vegetable ghee, sugar, and various others such as oil mills, paper production, and pharmaceuticals.

In this study, the Sentinel-1 and Sentinel-2 data was used along with ground truth information for crop classification by applying a Random Forest classifier (Figure 2).

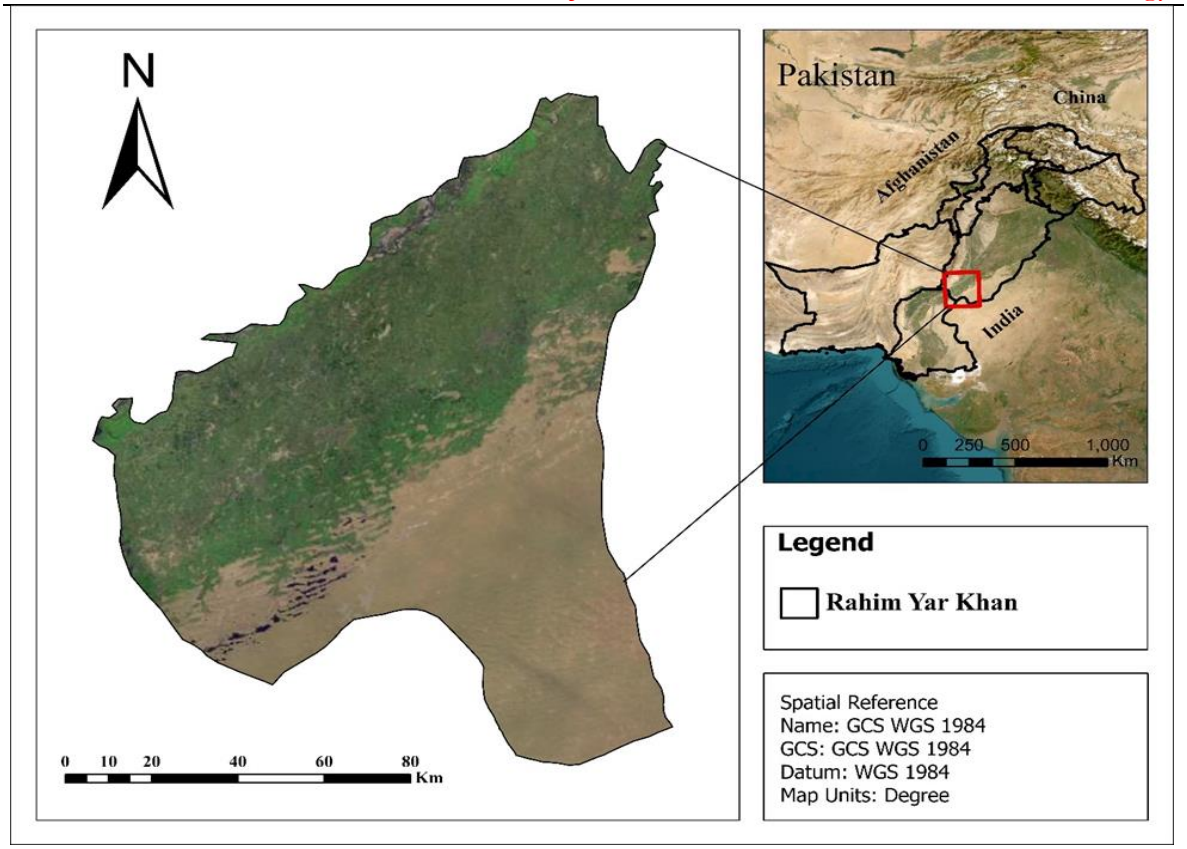

Figure 1: The Study area map of District Rahim Yar Khan

Satellite Data Used:

This study utilized the ground range detected (GRD) product from Sentinel-1A in Interferometric Wide (IW) mode with a fine 10 m spatial resolution. This data source offers two primary polarization channels: VV (cross-polarization) and VH (cross-polarization) in the Google Earth Engine (GEE) [12]. The images were acquired in whole kharif crop growing season, from May to October 2022, from planting to harvesting were for crop mapping. Likewise, the multispectral optical imagery of Sentinel-2 was used. The Sentinel-2 image has 13 spectral bands in visible, near-infrared (NIR), and Short-wave infrared (SWIR) region of the electromagnetic spectrum (Table 1). The spatial resolutions range from 10 to 60 meters. Sentinel-2 has frequent revisits, 10 days with one satellite and 5 days with two satellites [2]. The Sentinel-2, optical images, of Rahim Yar Khan with minimal cloud cover (less than 10%) and acquired between early May to October 2022 were used for analysis. Cloudy pixels were masked using Quality Assessment band and median reduction image applied to produce seasonal composite image to use with time series. Widely used vegetation indices, including the Normalized Difference Vegetation Index (NDVI) [16], Soil-Adjusted Vegetation index (SVI) [17], Bare Soil Index (BSI) [18], and Enhanced Vegetation Index (EVI) [16].

$$\mathrm{NDVI} = \frac{\mathrm{NIR}_\sigma - \mathrm{Red}_\sigma}{\mathrm{NIR}_\sigma + \mathrm{Red}_\sigma} \quad (1)$$

$$\mathrm{SAVI} = \frac{(\mathrm{NIR}_\sigma - \mathrm{REd}_\sigma)}{(\mathrm{NIR}_\sigma - \mathrm{Red}_\sigma + \mathrm{L})} \times (1 + \mathrm{L}) \quad (2)$$

$$\mathrm{BSI} = \left(\frac{(\mathrm{PRED}_\sigma + \mathrm{PSWIR1}_\sigma) - (\mathrm{PNIR}_\sigma + \mathrm{PBLUE}_\sigma)}{(\mathrm{PRED}_\sigma + \mathrm{PSWIR1}_\sigma) + (\mathrm{PNIR}_\sigma + \mathrm{PBLUE}_\sigma)}\right) + 1 \quad (3)$$

$$\mathrm{EVI} = 2.5 = \left(\frac{\mathrm{NIR}_\sigma - \mathrm{REd}_\sigma}{(\mathrm{NIR}_\sigma + 6\mathrm{red} - 7.5\ \mathrm{Blue}) + 1}\right) \quad (4)$$

Where $\mathrm{PBLUE}_\sigma, \mathrm{NIR}_\sigma$ and Red_σ represents reflectance in the blue, NIR and red wavebands, respectively.

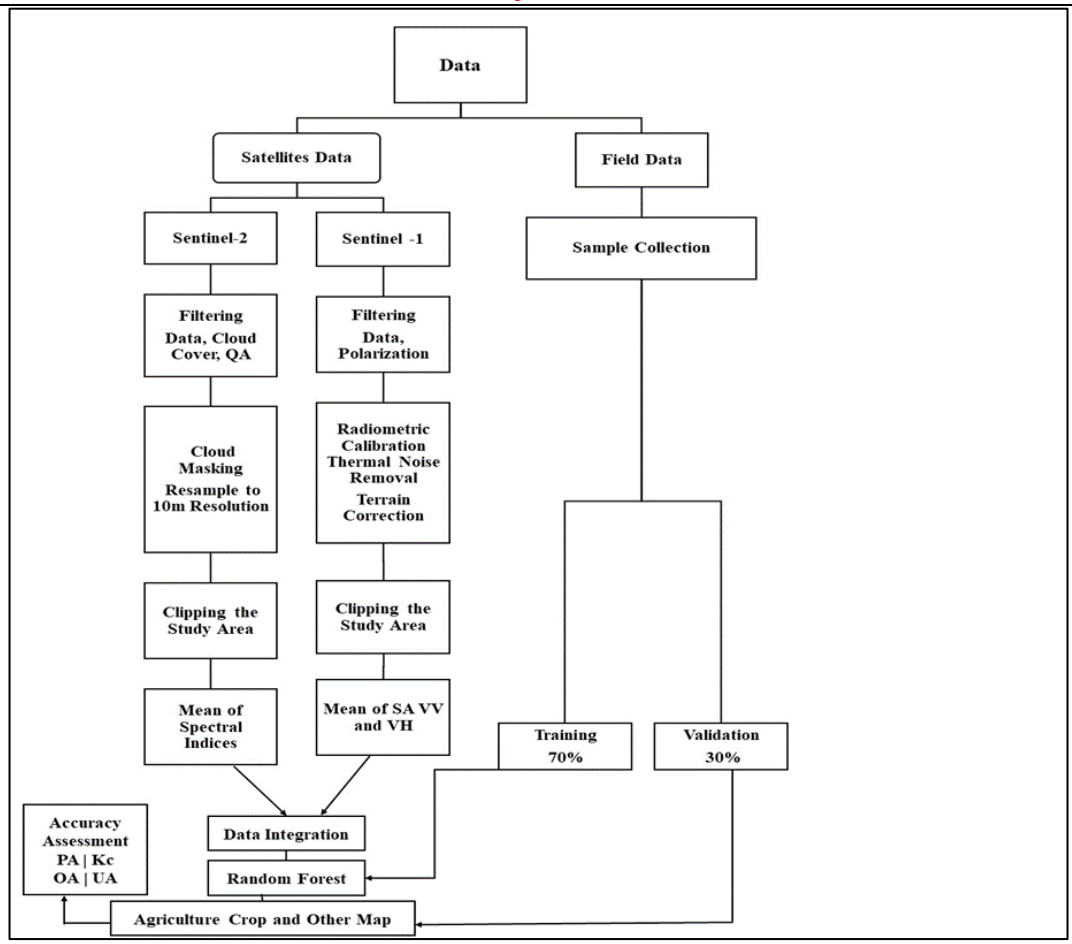

Figure 2: Flowchart of Crop Classification Using Random Forest Algorithm

Table 1: Characteristics of both Sentinel 1 and Sentinel 2 Sensors used in this Study.

Satellite	Band No	Wavelength(nm)	Band Name	Resolution (m)
Sentinel-1		C-band	VV	10
			VH	10
	2	490	Blue	10
	3	560	Green	10
	4	665	Red	10
Sentinel-2	8	842	Near-infrared	10
	11	1610.4	SWIR	20
	12	2202.4	SWIR	20

Ground Truth Information and Sample Data:

While crops were the primary emphasis; the study addressed regional heterogeneity and other misclassifications by defining broad LCLU groups. The LCLU categories included Barren, Built-up, Water Bodies, Cotton, Orchard, Rice, Sugarcane and Other Crops (Table 2) as well as (Figure 3). To evaluate a supervised classification Performance for crop mapping, reference samples from the 2022 growing seasons were obtained from May to September. These details enable the evaluation, modelling, and quantification of agricultural crop productivity. To train and evaluate the supervised classification system of crop mapping for Rahim Yar Khan, reference samples were divided in training and validation samples (70%, 30%). The agricultural crop was the primary focus of this study, however, because of the spatial variability of this region, the existence of different other land cover classes could have an impact on the outcomes of crop mapping. The study area's grassland is made up of all the small plants cultivated there, whereas the built-up consists of dwellings and impermeable surfaces. All the uncultivated area

is bare land. Water bodies in the research region include lakes, rivers, streams, and other bodies of still water. Any class that isn't included within one of the class categories (vegetation, other crops, forest, etc.) is referred to as an "other". Based on visually analyzing the multi-sensor composites and Google Earth geo-referenced images, the classes were determined on-screen. In addition to the locations of the sugarcane, cotton, rice, and orchard samples, a further training sample and validation points were also chosen randomly. To create a polygon to encompass each sampling point, on-screen digitizing was performed. Corresponding to the target crops, identified seven major groups of land use with land cover within the area of interest were utilized.

Table 2: Distribution of training and validation samples for LCLU classification in the study area

No	LCLU Class	Count	Training Sample	Validation Sample
1	Barren	102	71	31
2	Built up	119	83	36
3	Cotton	100	70	30
4	Orchard	100	70	30
5	Other Crop	108	75	33
6	Rice	100	70	30
7	Sugarcane	242	170	72
8	Water-bodies	101	70	31

The table 2 shows that approximately 70% of the obtained field samples were used to train classification models using approaches such as Random Forest, which were chosen for their ability to perform multi-class classification tasks and handle non-linear data relationships. The remaining 30% of field samples were set aside for model validation, with the data utilized to create agriculture crop and other land cover maps that serve as ground truth standards for assessing model correctness.

Random Forest Algorithm:

Random Forest (RF) is an ensemble classifier that uses numerous decision trees to address the limitations of single decision trees [19]. By using tune function random parameters are selected. In the present investigation, the ideal number of predictors/features (max features) was computed as the square root of the total number of available features, and it was determined that the ideal number of trees (mtry) was 100. One of RF's advantages is its capacity to identify important data inside each feature. A global optimum could be reached by including numerous trees, solving any issues that may have been brought on by a single tree. With this classifier, a vast amount of data may be classified effectively while handling uneven input features [20]. The best results are produced by RF classifiers in terms of effectiveness and accuracy. Mostly, the sample data are divided into two parts: one is training datasets for model construction and the second is test datasets for model confirmation [12]. It has been frequently used in the agricultural field. One of its drawbacks is that it makes trees difficult to envision because there are so many of them [21]. The RF classifier from GEE was used to obtain the LCLU classification from the Sentinel-1 (VV), Sentinel-1 (VH), Sentinel-1 (VV+VH) optical multispectral bands Sentinel-2, and integrated datasets of Sentinel-1 and Sentinel-2.

Accuracy Assessment:

Accuracy assessment of the LCLU is an important part of the classification procedure [22]. The degree of agreement among the outcomes and the values presumptively true is a common way to gauge accuracy [23]. All the classification outcomes were evaluated using confusion matrices to measure their overall accuracy (OA) (Eq 5), producer accuracy (PA), user accuracy (UA), the kappa coefficient (Eq 6), and F1-score (Eq 7) [22]. The overall accuracy indicates the number of accurately categorized reference pixels divided by all the references pixels.

$$\left(OA = \frac{\sum \text{correct predictions}}{\text{total number of predictions}}\right) \quad (5)$$

In Equation 6 predictions were calculated for all available validation samples and second, the predicted labels were compared to the true labels [8].

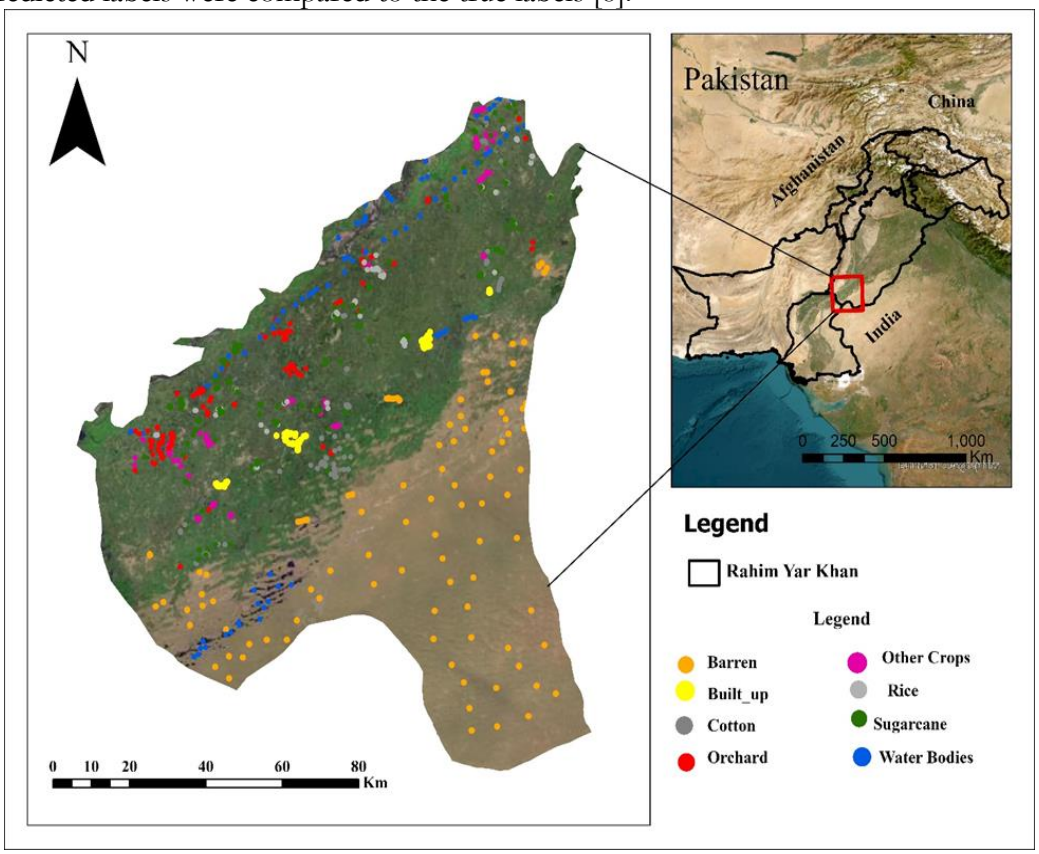

Figure 3: Sample Area of Rahim Yar Khan District

$$\text{Kappa Coefficient (KC)} = N\sum ri = 1xii - \sum ri = 1(xi + x + i)N2 - \sum ri = (xi + x + i) \quad (6)$$

Classified maps were evaluated using the F1-Score method, Eq (7), which calculates accuracy assessment statistics for each class and measures accuracy determined by the confusion matrices. The harmonic mean of recall and precision, two essential measures used to gauge both user accuracy and producer accuracy, is utilized to calculate the F1 score[24]. In comparison to independent producer and user indicators, it is an important signal for assessing the categorization model.

$$F1 = \frac{2 \times PA \times UA}{PA + UA} \quad (7)$$

Where PA represent the producer's accuracy whereas UA represent the user's accuracy

Result and Discussion:

By integrating Sentinel-2 and Sentinel-1 satellite data agricultural crops were mapped at 10-meter resolution for the Rahim Yar Khan district by using RF machine learning method in a cloud computing platform, Google Earth Engine (GEE). Multispectral data from Sentinel-2 and VV and VH cross polarizations from the Sentinel-1 was used for classifying crops. These maps accurately depict cropland and various land cover types, demonstrating the effectiveness of current approach in categorizing different crops like sugarcane, cotton, rice, orchards, water bodies, deserts and built-up areas. Various combinations of optical Sentinel-2 and microwave Sentinel-1 were tested using RF for classification of crops (Table 3). These combinations of satellite data include optical bands from Sentinel-2, VH polarization band from Sentinel-1, VV polarization band from Sentinel-1, combination of VH and VV polarization bands from

Sentinel-1, and combination optical bands from Sentinel-2 VH and VV polarization bands from Sentinel-1. Area statistics of different crops from Crop Reporting Service (CRS) for the year 2022 was used as reference for comparison with satellite based predicted crops.

Table 3: Area of different crops (in km^2) predicted by using different combination of Sentinel-1 and Sentinel-2 imagery and crop area from crop reporting service for the year 2022.

Class Name	Sentinel-2	Sentinel-1 VH	Sentinel-1 VV	Sentinel-1 VH+VV	Combined Multi-sensor Year 2022	CRS 2022
Sugarcane	1762.7	2581.4	3290.3	2707.1	1834.7	2165.0
Cotton	1717.6	1355.6	836.3	1474.2	1578.6	1897.9
Rice	212.3	989.4	835.7	781.6	204.4	283.2
Other Crop	2450.2	1695.9	1588.5	1704.9	2891.5	834.2
Orchard	58.5	199.4	213.9	137.1	54.31	196
Water Bodies	502.2	587.1	388.7	360.3	305.4	-
Desert	5386.6	4942.8	5088.2	5231.3	5524.0	-
Built up	504.3	234.0	343.9	189.1	192.8	-

Table 3 shows that the combination of Sentinel-1 and Sentinel-2 outputs area of sugarcane of 1834.71 km², which is quite close to the sugarcane area estimated from CRS with the value of 2165.07 km². For the other combination of bands, there is a large difference between satellite-based estimation of crop area and CRS crop area. Similarly, for the other crops cotton and rice, satellite-based area of crops using combination of sentinel-1 and sentinel-2 are quite close to CRS estimated as shown in Table 3.

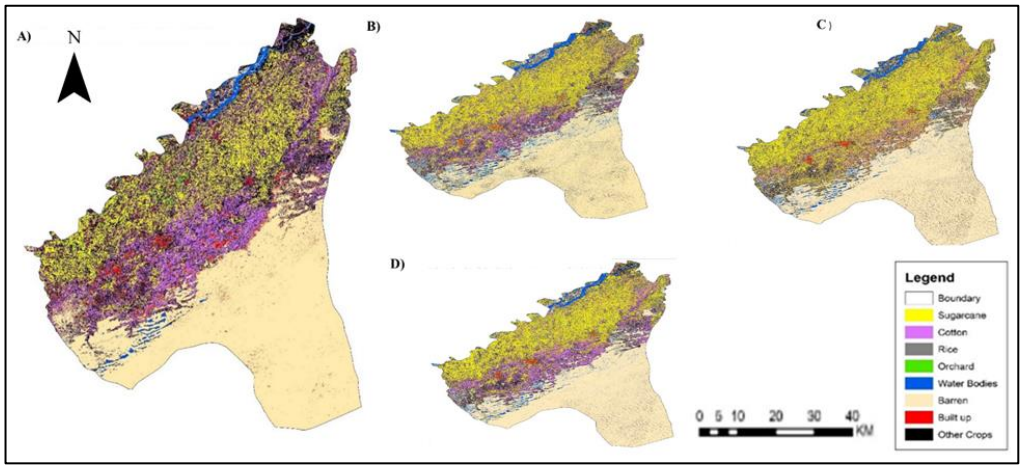

Figure 4: Classified maps of Rahim Yar Khan District using Sentinel-1 and Sentinel-2 (A)Crop Classification using Sentinel 2 Sensor Only (B) Crop Classification using Sentinel 1 VH Channel (C) Crop Classification using Sentinel 1 VV Channel (D) Crop Classification using Sentinel-1 VH +VV Channel.

To evaluate the accuracy of integration of different combination of Sentinel-1 and Sentinel-2 for crop classification using RF, different accuracy evaluation metrics were used such as overall accuracy (OA), F1-score, Kappa coefficient (KC), user's accuracy (UA), and producer's accuracy (PA) for key crops (sugarcane, rice, cotton, orchards) and other land cover types in Rahim Yar Khan District. Our results indicate high values of F1-score, user accuracy and producer accuracy for the scenario combining Sentinel-1 and Sentinel-2 data as compared to other four combinations (Table 4)

Promising results have been obtained when agricultural crops in the Rahim Yar Khan district were mapped at a 10-meter resolution using integration of Sentinel-2 and Sentinel-1 with the Random Forest (RF) machine learning approach in GEE platform. The study created precise maps that accurately depicted crops and different types of land cover by merging multispectral data from Sentinel-2 with VV and VH cross polarizations bands from Sentinel-1. The method

effectively classified several land cover types, including water bodies, deserts, and populated regions, in addition to various crops, including rice, cotton, sugarcane, and orchards. This illustrates how well the approach distinguishes and categorizes agricultural areas.

Table 4: Accuracy of Random Forest Algorithm Using Different Datasets on District Rahim Yar Khan

RF 2022 over			Sugarcane	Cotton	Rice	Other crops	Orchard	Water Bodies	Barren	Built up	OA	KC
RF VH	PA (%)		0.85	0.91	0.53	0.51	0.25	0.64	0.83	0.63		
	UA (%)		0.54	0.78	0.78	0.75	0.42	0.78	0.71	0.82	0.66	0.60
	F Score		0.66	0.84	0.63	0.61	0.31	0.70	0.76	0.71		
RF VV	PA (%)		0.82	0.5	0.39	0.27	0.25	0.75	0.83	0.86		
	UA (%)		0.45	0.63	0.61	0.36	0.72	0.80	0.80	1.0	0.62	0.58
	F Score		0.58	0.55	0.47	0.31	0.37	0.77	0.81	0.92		
RF VH+VV	PA (%)		0.91	0.91	0.53	0.48	0.25	0.67	0.93	0.88		
	UA (%)		0.56	0.78	0.93	0.7	0.61	0.90	0.77	0.94	0.72	0.67
	F Score		0.69	0.84	0.68	0.57	0.35	0.77	0.84	0.91		
RF 2022 over Sentinel-2	PA (%)		0.98	0.95	0.82	0.86	0.59	0.96	0.93	0.97		
	UA (%)		0.77	0.88	1.0	0.89	0.95	1.0	0.96	0.94	0.89	0.87
	F Score		0.86	0.91	0.90	0.87	0.73	0.98	0.94	0.95		
RF 2022 Combined Multi-Sensor	PA (%)		1.0	1.0	0.78	0.87	0.62	1.0	1.0	0.86		
	UA (%)		0.96	0.88	1.0	0.96	1.0	1.0	1.0	1.0	0.93	0.90
	F Score		0.87	0.94	0.88	0.90	0.76	1.0	1.0	1.0		

A comparative study conducted with Crop Reporting Service (CRS) data for 2022 confirmed that the satellite-based forecasts were accurate. Particularly for rice, cotton, and sugarcane, the crop area estimates produced by combining Sentinel-1 and Sentinel-2 data closely matched the CRS data. For example, the estimated area of sugarcane was 1834.71 km², which is in good agreement with the 2165.07 km² estimate from the CRS. Significant differences were shown by other combinations of satellite data, highlighting the integrated approach's superiority for precise crop area calculation.

Sentinel-1 and Sentinel-2 data combined approach consistently produced high values for all of the accuracy evaluation criteria used in the study, overall accuracy (OA), F1-score, Kappa coefficient (KC), user's accuracy (UA), and producer's accuracy (PA). These results demonstrate how land cover categorization and agricultural monitoring might be enhanced by combining cutting-edge machine learning algorithms with optical and microwave satellite data. This would offer a dependable resource management and planning tool for agricultural regions.

The study's conclusions, which include timely and precise crop categorization maps, greatly improve agricultural management. Farmers may increase yields and resource efficiency by using these maps to help them plan their planting, irrigation, and harvesting operations. For food security initiatives, this study offers a scalable and affordable way to reliably monitor and estimate crop output. In order to prevent food shortages, early identification of regions at risk for low yields or crop failure enables immediate action. Accurate crop mapping also facilitates resilient agricultural practices and policies for long-term food security by tracking agricultural patterns and evaluating the effects of climate change.

Conclusion:

The use of remote sensing (RS) has expanded rapidly in recent years because of the availability of high spatial resolution Sentinel-2 and Sentinel-1 free of cost at high temporal resolution and high-performance cloud computing platforms like GEE for processing and analysis of massive amounts of data. This study demonstrates the use of state-of-the-art machine learning method RF and fusion of Sentinel 2 and Sentinel 1 produces a crop classification map at high accuracy as compared to traditional statistical classification methods and only single satellite-based data. The main goal of the research was to map and classification of crop cover in Pakistan's, district Rahim Yar Khan. Different combination of satellite data including optical bands from Sentinel-2, VH polarization band from Sentinel-1, VV polarization band from Sentinel-1, combination of VH and VV polarization bands from Sentinel-1, and combination optical bands from Sentinel-2 and VH and VV polarization bands from Sentinel-1 were testing to select which combination would provide high accuracy. Our results show combination of Sentinel-1 and Sentinel-2 outperforms as compared to individual use of optical and SAR imagery. For the future research very high-resolution imagery such as World View, GeoEye, and Pleiades can be used with other machine learning methods like support vector machine and artificial neural network for better accuracy of crop classification.

Acknowledgement:

I would like to express my sincere gratitude to the Crop Reporting Services for their essential contribution to this study. We are also thankful for the cooperation of the Urban Unit which significantly contributed to the success of this research. Additionally, I extend my appreciation to the European Space Agency for providing access to Sentinel-1 and Sentinel-2 satellite imagery, which played a crucial role in the analysis and classification of crops.

Author's Contribution:

All the authors had different contributions to this research work and are mentioned here accordingly. Conceptualization (S.A, M.U), formal analysis (F.U, A.A), methodology (M.U, F.U, A.A and S.A), writing—original draft preparation (F.U, Z.A.A, A.A, S.A), writing—review and editing (S.A, A.A, Z.A.A, M.U, S.M.I), visualization (S.U.K and S.M.I) All authors have read and agreed to the published version of the manuscript.

Conflict of Interest: The authors declare they have no conflict of interest in publishing this manuscript in this Journal.

References:

[1] Asia and the Pacific Regional Overview of Food Security and Nutrition 2022. FAO, 2023. doi: 10.4060/cc3990en.

[2] G. A. Abubakar et al., "Mapping Maize Cropland and Land Cover in Semi-Arid Region in Northern Nigeria Using Machine Learning and Google Earth Engine," Remote Sens., vol. 15, no. 11, p. 2835, May 2023, doi: 10.3390/rs15112835.

[3] M. Majeed et al., "Prediction of flash flood susceptibility using integrating analytic hierarchy process (AHP) and frequency ratio (FR) algorithms," Front. Environ. Sci., vol. 10, no. January, pp. 1–14, 2023, doi: 10.3389/fenvs.2022.1037547.

[4] J. Wang et al., "Mapping sugarcane plantation dynamics in Guangxi, China, by time series Sentinel-1, Sentinel-2 and Landsat images," Remote Sens. Environ., vol. 247, p. 111951, Sep. 2020, doi: 10.1016/j.rse.2020.111951.

[5] V. Tiwari et al., "Wheat Area Mapping in Afghanistan Based on Optical and SAR Time-Series Images in Google Earth Engine Cloud Environment," Front. Environ. Sci., vol. 8, Jun. 2020, doi: 10.3389/fenvs.2020.00077.

[6] Y. Durgun, A. Gobin, R. Van De Kerchove, and B. Tychon, "Crop Area Mapping Using 100-m Proba-V Time Series," Remote Sens., vol. 8, no. 7, p. 585, Jul. 2016, doi: 10.3390/rs8070585.

[7] A. Elders et al., "Estimating crop type and yield of small holder fields in Burkina Faso using multi-day Sentinel-2," Remote Sens. Appl. Soc. Environ., vol. 27, p. 100820, Aug. 2022, doi: 10.1016/j.rsase.2022.100820.

[8] K. Van Tricht, A. Gobin, S. Gilliams, and I. Piccard, "Synergistic Use of Radar Sentinel-1 and Optical Sentinel-2 Imagery for Crop Mapping: A Case Study for Belgium," Remote Sens., vol. 10, no. 10, p. 1642, Oct. 2018, doi: 10.3390/rs10101642.

[9] Y. Pageot, F. Baup, J. Inglada, N. Baghdadi, and V. Demarez, "Detection of Irrigated and Rainfed Crops in Temperate Areas Using Sentinel-1 and Sentinel-2 Time Series," Remote Sens., vol. 12, no. 18, p. 3044, Sep. 2020, doi: 10.3390/rs12183044.

[10] G. R. Aduvukha et al., "Cropping Pattern Mapping in an Agro-Natural Heterogeneous Landscape Using Sentinel-2 and Sentinel-1 Satellite Datasets," Agriculture, vol. 11, no. 6, p. 530, Jun. 2021, doi: 10.3390/agriculture11060530.

[11] S. Felegari et al., "Integration of Sentinel 1 and Sentinel 2 Satellite Images for Crop Mapping," Appl. Sci., vol. 11, no. 21, p. 10104, Oct. 2021, doi: 10.3390/app112110104.

[12] C. Li et al., "Mapping Winter Wheat with Optical and SAR Images Based on Google Earth Engine in Henan Province, China," Remote Sens., vol. 14, no. 2, Jan. 2022, doi: 10.3390/rs14020284.

[13] S. Asam, U. Gessner, R. Almengor González, M. Wenzl, J. Kriese, and C. Kuenzer, "Mapping Crop Types of Germany by Combining Temporal Statistical Metrics of Sentinel-1 and Sentinel-2 Time Series with LPIS Data," Remote Sens., vol. 14, no. 13, p. 2981, Jun. 2022, doi: 10.3390/rs14132981.

[14] N. Gorelick, M. Hancher, M. Dixon, S. Ilyushchenko, D. Thau, and R. Moore, "Google Earth Engine: Planetary-scale geospatial analysis for everyone," Remote Sens. Environ., vol. 202, pp. 18–27, Dec. 2017, doi: 10.1016/j.rse.2017.06.031.

[15] W. Zhang, M. Brandt, A. V. Prishchepov, Z. Li, C. Lyu, and R. Fensholt, "Mapping the Dynamics of Winter Wheat in the North China Plain from Dense Landsat Time Series (1999 to 2019)," Remote Sens., vol. 13, no. 6, p. 1170, Mar. 2021, doi: 10.3390/rs13061170.

[16] A. Huete, K. Didan, T. Miura, E. . Rodriguez, X. Gao, and L. . Ferreira, "(NDVI EVI)Overview of the radiometric and biophysical performance of the MODIS

vegetation indices," Remote Sens. Environ., vol. 83, no. 1–2, pp. 195–213, Nov. 2002, doi: 10.1016/S0034-4257(02)00096-2.

[17] A. . Huete, "A soil-adjusted vegetation index (SAVI)," Remote Sens. Environ., vol. 25, no. 3, pp. 295–309, Aug. 1988, doi: 10.1016/0034-4257(88)90106-X.

[18] N. Mzid, S. Pignatti, W. Huang, and R. Casa, "An Analysis of Bare Soil Occurrence in Arable Croplands for Remote Sensing Topsoil Applications," Remote Sens., vol. 13, no. 3, p. 474, Jan. 2021, doi: 10.3390/rs13030474.

[19] Y. He, E. Lee, and T. A. Warner, "A time series of annual land use and land cover maps of China from 1982 to 2013 generated using AVHRR GIMMS NDVI3g data," Remote Sens. Environ., vol. 199, pp. 201–217, Sep. 2017, doi: 10.1016/j.rse.2017.07.010.

[20] V. F. Rodriguez-Galiano, B. Ghimire, J. Rogan, M. Chica-Olmo, and J. P. Rigol-Sanchez, "An assessment of the effectiveness of a random forest classifier for land-cover classification," ISPRS J. Photogramm. Remote Sens., vol. 67, pp. 93–104, Jan. 2012, doi: 10.1016/j.isprsjprs.2011.11.002.

[21] L. Breiman, "machine Learning," Mach. Learn., vol. 45, no. 1, pp. 5–32, 2001, doi: 10.1023/A:1010933404324.

[22] A. F. Koko, Y. Wu, G. A. Abubakar, A. A. N. Alabsi, R. Hamed, and M. Bello, "Thirty Years of Land Use/Land Cover Changes and Their Impact on Urban Climate: A Study of Kano Metropolis, Nigeria," Land, vol. 10, no. 11, p. 1106, Oct. 2021, doi: 10.3390/land10111106.

[23] A. Tassi and M. Vizzari, "Object-Oriented LULC Classification in Google Earth Engine Combining SNIC, GLCM, and Machine Learning Algorithms," Remote Sens., vol. 12, no. 22, p. 3776, Nov. 2020, doi: 10.3390/rs12223776.

[24] D. Chicco and G. Jurman, "The advantages of the Matthews correlation coefficient (MCC) over F1 score and accuracy in binary classification evaluation," BMC Genomics, vol. 21, no. 1, p. 6, Dec. 2020, doi: 10.1186/s12864-019-6413-7.